# Vacuum electron field emission from $SnO_2$ nanowhiskers annealed in $N_2$ and $O_2$ atmospheres

Suhua Luo,[a] Paul K. Chu,[b] and Zengfeng Di[a]
*Department of Physics and Materials Science, City University of Hong Kong, Tat Chee Avenue, Kowloon, Hong Kong, China*

Miao Zhang, Weili Liu, and Chenglu Lin
*Research Center of Semiconductor Functional Film Engineering, Shanghai Institute of Microsystem and Information Technology, Chinese Academy of Sciences, Shanghai 200050, China*

Jiyang Fan and Xinglong Wu
*Department of Physics and Materials Science, City University of Hong Kong, Tat Chee Avenue, Kowloon, Hong Kong and National Laboratory of Solid State Microstructures and Department of Physics, Nanjing University, Nanjing 210093, China*

(Received 26 October 2005; accepted 5 December 2005; published online 5 January 2006)

The field emission properties of $SnO_2$ nanowhiskers were observed to change after annealing under $O_2$ and $N_2$. The electron current increased significantly from the sample annealed in $N_2$ and the threshold field decreased from 3.17 V/$\mu$m of the as-grown sample to 2.59 V/$\mu$m of the annealed sample. The mechanism of the field emission enhancement was explored using Fourier transform infrared spectroscopy and x-ray photoelectron spectroscopy (XPS). The results reveal that after annealing in $N_2$, the amount of Sn–O bonds decreased and N atoms were introduced onto the surface. The binding energies of Sn 3*d* and O 1*s* determined by high resolution XPS analysis show a shift of 0.55 and 0.47 eV, respectively, toward the high energy side. This shows that the electron emission enhancement arises from a decrease in the work function. The changes in the field emission effect from the sample annealed in $O_2$ are different and a possible mechanism is also proposed. © *2006 American Institute of Physics*. [DOI: 10.1063/1.2161573]

Materials displaying field emission have attracted much interest because of their potential applications as cathodes in field emission displays (FEDs). One-dimensional (1D) nanostructures with high aspect ratios such as carbon nanotubes (CNT)[1,2] are projected to be the ideal field-emission (FE) electron sources. Recently, the field emission properties of III-V and IV-IV nanowires[3,4] and some oxide systems, such as zinc oxide[5] and indium oxide,[6] have also become a subject of experimental investigation. Tin oxide is useful in display devices as an anode and in gas sensors, transparent conducting electrodes, and dye-based solar cells.[7–10] Together with other inherent properties including thermal stability, oxidation resistance, as well as large aspect ratio, one-dimensional $SnO_2$ nanostructures are potential FE materials.

Although our previous work has shown that $SnO_2$ nanowhiskers are good electron emitters,[11] the effects of the surface states, which are important to a good understanding of the electron emission mechanism, are, however, unclear. The surfaces of $SnO_2$ nanowhiskers are very active with regard to chemisorption of oxygen and other atoms due to the variable valence bands of Sn, thereby providing a useful way to change the surface chemistry by surface oxidation or introduction of surface defects.[12] Such surface modification leads to the rearrangement of the host atoms at the near surface thus changing the band structure of the $SnO_2$ nanowhisker system. Thermal treatment in different gas ambients is an easy and effective way to introduce different atoms onto the surface, and past studies have shown that the annealing environment strongly impacts the structure of the $SnO_2$ nanoparticles.[13] In this study, $SnO_2$ nanowhiskers were annealed in $O_2$ and $N_2$, and the field emission characteristics were investigated in comparison with the as-grown nanowhiskers. Fourier transform infrared spectroscopy (FTIR) and x-ray photoelectron spectroscopy (XPS) were employed to monitor the changes in the chemical bonds and atomic binding states at the surface of the $SnO_2$ nanowhiskers. The electron emission mechanism of the nanowhiskers is formulated based on the experimental results.

$SnO_2$ nanowhiskers were prepared by thermal evaporation of metallic tin and the fabrication conditions have been described elsewhere.[11] In order to ensure the reliability of the results, after the as-grown samples (sample A) underwent field-emission measurements in vacuum, annealing ensued in $O_2$ (sample B) and $N_2$ (sample C) at 600 °C. After annealing, the samples were immediately loaded into the field emission test chamber with a base vacuum better than $5 \times 10^{-6}$ Pa. The samples (about $7 \times 8$ mm$^2$) were affixed on a stainless-steel support to serve as the cathode. A parallel phosphor screen (anode) located at a distance of 200 $\mu$m served as the anode.

The dependence of the emission current density $J$ obtained by dividing the measured current by the total apparent area of the substrate on which the emitters are grown on the applied electric field ($E$) is shown in Fig. 1(a). Relatively smooth and consistent $J$-$E$ curves are obtained indicating the robustness of the emission process from our samples. The insets show the spatial distribution images of the luminescent spots on the anode of sample C at the emission fields of 4.2

[a]Also at: Research Center of Semiconductor Functional Film Engineering, Shanghai Institute of Microsystem and Information Technology, Chinese Academy of Sciences, Shanghai 200050, China.
[b]Author to whom correspondence should be addressed; electronic mail: paul.chu@cityu.edu.hk

 

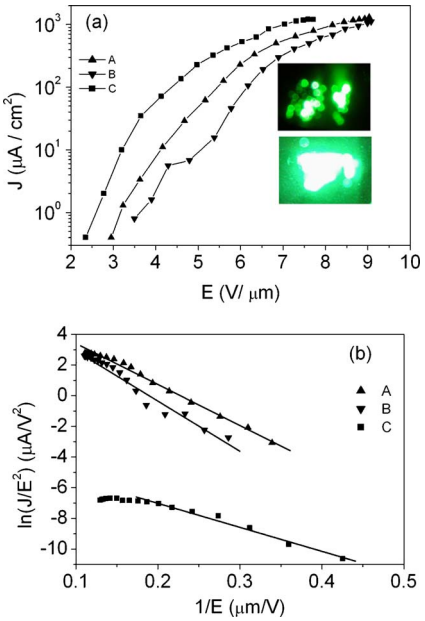


FIG. 1. (Color online) (a) Field-emission current density-field curves; (b) Fowler-Nordheim plots for both the as-grown and annealed $SnO_2$ nanowhiskers.

and 7.5 V/$\mu$m. The anode is lightened unevenly at 4.2 V/$\mu$m. When the field is increased to 7.5 V/$\mu$m, the anode illuminates homogeneously and brightly showing the saturated emission current. The Fowler-Nordheim (*F-N*) plots corresponding to the data in Fig. 1(a) are shown in Fig. 1(b). It exhibits a linear relationship in the range below the saturation current, indicating that the field emission process from the nanostructured $SnO_2$ is a barrier tunneling, quantum mechanical process (*F-N* tunneling).[14]

The electron emission current of the $SnO_2$ nanowhiskers is enhanced after annealing in $N_2$ but decreases slightly after annealing in $O_2$. The turn-on fields defined as the field required to detect a current of 1 $\mu$A/cm$^2$ are 3.17, 3.63, and 2.59 V/$\mu$m and reach 1 mA/cm$^2$ at 8.19, 8.95, and 7.04 V/$\mu$m for samples A, B, and C, respectively. The turn-on and threshold fields are comparable to the best-reported data of carbon nanotubes[1–3] and the tetrapod-shaped ZnO nanostructures.[15]

It is important to elucidate the mechanisms responsible for the field emission property changes of the $SnO_2$ nanowhiskers. The field emission current density $J$ can be expressed as a function of the applied electric field $E$, the local work function of the emission tip $\Phi$, and a geometric enhancement factor $\beta$ to be $J \propto (\beta^2\Phi)E^2\exp[B\Phi^{3/2}/(\beta E)]$, where $B$ is a constant.[16] The parameters that govern the emission are the effective work function $\Phi$ and geometric enhancement factor $\beta$. For bulk $SnO_2$, $\Phi$ is estimated to be 4.3 eV.[17] Hence, it is not a good field emitter. On the other hand, the one-dimensional (1D) nanostructure has a big field enhancement factor that reduces the minimal field required for effective electron emission. Moreover, the as-grown $SnO_2$ nanostructure is a *n*-type semiconductor and therefore a good conductive material for electrons. The parameter $\beta$ describes how the electric field can be enhanced by protrusions from the emitting surface. In the *F-N* coordinates, the above equation becomes $\ln(J/E^2) \propto 1/E$, and the slope of the *F-N* plot is given by $S=-sB\Phi^{3/2}/\beta$, where $s$ is a slope correction factor. The slopes determined from samples A, B, and C are −24.8, −32, and −16.2, respectively [Fig. 1(b)]. It suggests an increase/decrease in work function for samples B/C compared to the as-prepared sample, since the field enhancement factor $\beta$ is nearly the same for these samples. As aforementioned, the emission is a barrier tunneling, quantum mechanical process. The electron field emission process involves extraction of electrons from the tin oxide nanowhiskers by tunneling through the surface potential barrier to the vacuum state. Annealing the sample in different atmospheres may change the surface structure and result in different surface potential barriers. Therefore, the chemical bonding states at the surface of the nanowhiskers were characterized by Fourier transform infrared spectroscopy (FTIR) which may provide information about surface defects after annealing.

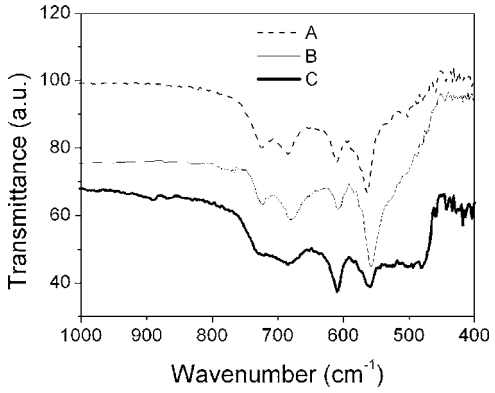


FIG. 2. FTIR spectra of both the as-grown and annealed $SnO_2$ nanowhiskers.

Rutile $SnO_2$ belongs to the space group $D_{4h}^{14}$ of which the normal lattice vibration at the $\Gamma$ point of Brillouin zone can be given on the basis of group theory by[18]

$$\Gamma = A_{1g} + A_{2g} + A_{2u} + B_{1g} + B_{2g} + 2B_{1u} + E_g + 3E_u,$$

where $A_{2u}$ and $E_u$ are active infrared vibration modes. The FTIR spectra acquired from the $SnO_2$ nanowhiskers are shown in Fig. 2. In these samples, the main variable peaks appear in the range of 400 and 800 cm$^{-1}$. All the samples exhibit two well-defined peaks at ~560 and ~610 cm$^{-1}$. Two relatively weak peaks centered at 680 and 726 cm$^{-1}$ can be observed from samples A and B. Sample B shows the strongest and sharpest absorption peaks out of the three samples, suggesting a crystal structure with the highest quality. The 558 cm$^{-1}$ absorption band of the $N_2$ or $O_2$ annealed sample shifts down by 6 cm$^{-1}$ compared to the as-grown sample. The 610 and 678 cm$^{-1}$ peaks can be assigned to the transverse and longitudinal $E_u$ modes, respectively. The two bands at 560 and 705 cm$^{-1}$ arise from the bending vibrations of O–Sn–O, which correspond to the $A_{2u}$ modes.[19] It can be observed that the intensities of these four absorption peaks in the spectrum of sample C decrease except for the 610 cm$^{-1}$ band. The 682 and 722 cm$^{-1}$ absorption bands transform into two broad shoulders while the 560 cm$^{-1}$ absorption band broadens and extends to 480 cm$^{-1}$. Obviously, annealing in $N_2$ destroys the surface stoichiometric structure and increases the structure disorder, thereby resulting in the broadened absorption bands.

To further investigate the mechanism, XPS measurements were performed on the same samples. Figures 3(a) and 3(b) show the high-resolution XPS spectra of both the as-

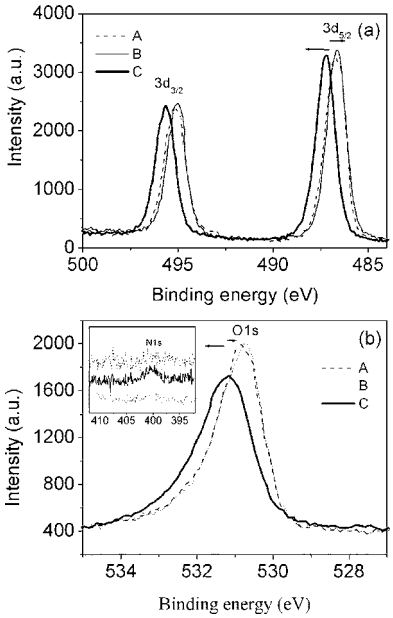


FIG. 3. High-resolution XPS spectra acquired from the as-grown and annealed $SnO_2$ nanowhiskers: (a) Sn 3*d* and (b) O 1*s* spectra. The insets in (b) are the N 1*s* spectra obtained from the as-grown and annealed $SnO_2$ nanowhiskers.

grown and annealed tin oxide nanowhiskers in the binding energy region corresponding to the Sn 3*d* and O 1*s* core levels. The peaks corresponding to the Sn 3*d* photoelectrons shift slightly toward lower binding energies in the sample annealed in $O_2$ and become sharper and stronger, while the peaks of the Sn 3*d* shift 0.55 eV higher in the sample annealed in $N_2$. With regard to O 1*s*, the peak behaves the same as that of Sn 3*d*. That is, the peaks shift 0.12 eV toward a lower binding energy in sample B but 0.47 eV toward a higher binding energy in sample C. The inset in Fig. 3(b) indicates the presence of the N 1*s* peak in sample C, showing clues that nitrogen is introduced after annealing in $N_2$. The atomic concentration ratios of O to Sn can be obtained by correcting the ratios of the O 1*s* and Sn 3*d* peak areas, which are 1.73, 1.76, 1.52 for samples A, B, and C, respectively, showing a 12% decrease in sample C. The full widths at half maxima (FWHM) of the Sn $3d_{5/2}$ spectra changed a little for all the samples, while the FWHM of the O 1*s* spectra changes largely in the sample annealed in $N_2$, increasing from 1.77 to 2.03 eV.

Considering the weakened and broadened absorption peaks in the FTIR spectra in sample C, the variations in the O 1*s* and Sn 3*d* spectra, the appearance of the N 1*s* peak, and the decrease in the O:Sn atomic ratio, it can be inferred that nitrogen is introduced into the surface of sample C to form N–O bonds. The weaker and broadened absorption bands at 682, 722, and 480 $cm^{-1}$ may be due to the local surface disorder caused by the new structure. The surface of sample B is reoxidized after annealing in $O_2$ and so the crystal quality is improved. As a result, the peaks are sharper.

It is important to note the peak of Sn 3*d* and O 1*s*. They shift 0.55 and 0.47 eV, respectively, toward higher binding energies in sample C. This means that the binding energy of the valence-band maximum (VBM) is also increased after annealing in $N_2$ and the decrease of VBM at the surface of the nanowhiskers suggests shifting of the Fermi level toward the vacuum level.[20] Consequently, the surface work function is reduced. That is, the potential barrier the electrons have to overcome in vacuum diminishes. However, in sample B, the Sn 3*d* and O 1*s* peaks shift toward lower binding energies, indicating the formation of a more stable structure that increases the surface potential barrier and weakens the field emission behavior. This is consistent with previous reports that surface treatment by laser irradiation or plasma exposure can change the surface potential barrier height and width.[21,22] Our experiments show that simple annealing in nitrogen can improve the field emission property of $SnO_2$ nanowhiskers.

In conclusion, the field emission characteristics of $SnO_2$ nanowhiskers annealed in $N_2$ and $O_2$ were investigated and compared to those of the as-grown ones. Analysis of the slope and intercept of the Fowler-Nordheim plots reveals that the dependence of the threshold field on the modified surface originates from the difference in the work function. Annealing in $N_2$ leaves the surface locally terminated with N–O bonds. This enhances emission through changing of the surface band structure thus decreasing the emission barrier or lowering the work function. Annealing in $O_2$ leaves a more chemically uniform surface and increases the emission barrier.

This work was financially supported by the City University of Hong Kong Direct Allocation Grant No. 9360110 and Science & Technology Committee of Shanghai (0359nm204 and 0252nm084).

[1] W. A. de Heer, A. Chatelain, and D. Ugarte, Science **270**, 1179 (1995).
[2] T. J. Vink, M. Gillies, J. C. Kriege, and H. W. van de Laar, Appl. Phys. Lett. **83**, 3552 (2003).
[3] D. Golberg, Y. Bando, L. Bourgeois, K. Kurashima, and T. Sato, Appl. Phys. Lett. **77**, 1979 (2000).
[4] P. Gröning, P. Ruffieux, L. Schlapbach, and O. Gröning, Adv. Eng. Mater. **5**, 541 (2003).
[5] Y. K. Tseng, C. J. Huang, H. M. Cheng, I. N. Lin, K. S. Liu, and I. C. Chen, Adv. Funct. Mater. **13**, 811 (2003).
[6] Hongbo Jia, Ye Zhang, Xihong Chen, Jing Shu, Xuhui Luo, Zhensheng Zhang, and Dapeng Yu, Appl. Phys. Lett. **82**, 4146 (2003).
[7] S. J. Laverty and P. D. Maguire, J. Vac. Sci. Technol. B **19**, 1 (2001).
[8] J. F. McAleer, P. Moseley, P. Bourke, J. O. W. Norris, and R. Stephan, Sens. Actuators **8**, 251 (1985).
[9] K. L. Chopra, S. Major, and D. K. Pandya, Thin Solid Films **102**, 1 (1983).
[10] S. Ferrere, A. Zaban, and B. A. Gsegg, J. Phys. Chem. B **101**, 4490 (1997).
[11] S. H. Luo, Q. Wan, W. L. Liu, M. Zhang, Z. F. Di, S. Y. Wang, Z. T. Song, C. L. Lin, and J. Y. Dai, Nanotechnology **15**, 1424 (2004).
[12] David F. Cox, Teresa B. Fryberger, and Steve Semancik, Phys. Rev. B **38**, 2073 (1988).
[13] Nicolas Sergent, Patrick Gélin, Laurent Périer-Camby, Hélène Praliaud, and Gérard Thomas, Sens. Actuators B **84**, 176 (2002).
[14] T. Sugino, C. Kimura, and T. Yamamoto, Appl. Phys. Lett. **80**, 3602 (2002).
[15] Q. Wan, C. L. Lin, X. B. Yu, and T. H. Wang, Appl. Phys. Lett. **84**, 124 (2004).
[16] R. G. Forbes and K. L. Jensen, Ultramicroscopy **89**, 17 (2001).
[17] A. C. Arias, L. S. Roman, T. Kugler, R. Toniolo, M. S. Meruvia, and I. A. Hümmelgen, Thin Solid Films **371**, 201 (2000).
[18] P. S. Peercy and Morosin, Phys. Rev. B **7**, 2779 (1973).
[19] R. S. Katiyar, P. Dawson, M. M. Hargreave, and G. R. Wilkinson, J. Phys. C **4**, 2421 (1971).
[20] Sang Youn Han, Jong Kyu Kim, Jong-Lam Lee, and Young-Joon Baik, Appl. Phys. Lett. **76**, 3694 (2000).
[21] J. S. Kim, K. S. Ahn, C. O. Kim, and J. P. Hong, Appl. Phys. Lett. **82**, 1607 (2003).
[22] C. H. Weng, K. C. Leou, H. W. Wei, Z. Y. Juang, M. T. Wei, C. H. Tung, and C. H. Tsai, Appl. Phys. Lett. **85**, 4732 (2004).